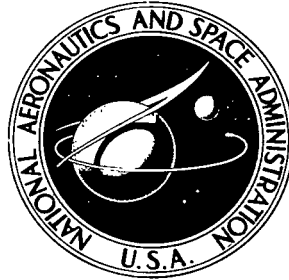


NASA TECHNICAL NOTE



NASA TN D-6394

2.1

NASA TN D-6394

LOAN COPY: RETURN TO
AFWL (DOGL)
KIRTLAND AFB, N. M.

0132928



POTENTIAL FLOW SOLUTION FOR A STOL WING PROPULSION SYSTEM

by James A. Albers and Merle C. Potter

Lewis Research Center

Cleveland, Ohio 44135



0132928

1. Report No. NASA TN D-6394	2. Government Accession No.	3. Recipient's Catalog No.	
4. Title and Subtitle POTENTIAL FLOW SOLUTION FOR A STOL WING PROPULSION SYSTEM	5. Report Date July 1971		6. Performing Organization Code
	7. Author(s) James A. Albers and Merle C. Potter		8. Performing Organization Report No. E-6132
9. Performing Organization Name and Address Lewis Research Center National Aeronautics and Space Administration Cleveland, Ohio 44135	10. Work Unit No. 721-03		11. Contract or Grant No.
	12. Sponsoring Agency Name and Address National Aeronautics and Space Administration Washington, D. C. 20546		13. Type of Report and Period Covered Technical Note
15. Supplementary Notes	14. Sponsoring Agency Code		
16. Abstract The analysis considers a two-dimensional wing-fan system which consists of an airfoil with flap; the fans, which have a distributed suction at their inlet and a jet at their exit; and a jet sheet leaving the flap trailing edge. The solution provides the incompressible potential flow for any value of fan or engine mass flow coefficient, the thrust coefficient for the propulsion system exhaust, and the wing and flap angle of attack. The report presents flow fields, pressure distributions, and lift coefficients for a particular, externally blown flap, high-lift configuration.			
17. Key Words (Suggested by Author(s)) Potential flow Airfoils STOL aircraft Pressure distribution Propulsion system Jet exhaust		18. Distribution Statement Unclassified - unlimited	
19. Security Classif. (of this report) Unclassified	20. Security Classif. (of this page) Unclassified	21. No. of Pages 34	22. Price* \$3.00



CONTENTS

	Page
SUMMARY	1
INTRODUCTION	1
ANALYSIS	3
Representation of Wing-Propulsion System	3
Basic Equations and Boundary Conditions	4
Formulation of the Boundary Condition as an Integral Equation	5
Solution of Integral Equation	6
Basic Solutions	8
Combination Solution	9
Location of Propulsion System Exhaust Jet	10
Inlet Air Suction	10
DISCUSSION	11
Validity of Analysis	11
Example Applications	12
CONCLUDING REMARKS	15
APPENDIXES	
A - SYMBOLS	16
B - CALCULATION OF FLOW QUANTITIES	18
REFERENCES	20

POTENTIAL FLOW SOLUTION FOR A STOL WING PROPULSION SYSTEM

by James A. Albers and Merle C. Potter*

Lewis Research Center

SUMMARY

The analysis considers a two-dimensional combined wing and propulsion system which consists of an airfoil (with flap) and fans located under the wing.

A numerical method is developed which includes the effect of suction at the inlet of the propulsion system and treats the exhaust jet as part of the solid body to determine its approximate location. The method provides the potential flow solution for any fan or engine mass flow coefficient, the thrust coefficient for the propulsion system exhaust, and the wing and flap angles of attack. Validity of the numerical solution for a case with suction (but with no jet) was indicated by application of the program to a two-dimensional inlet; excellent agreement was found with experimental results.

The analysis was used to obtain pressure distributions, flow fields, and lift coefficients for an externally blown flap, high-lift configuration. The flow field for this configuration indicated high upwash angles (60° to 90°) at the propulsion system inlet and large jet penetrations at high angles of attack. A comparison of two-dimensional lift coefficients obtained by the method of this report and Spence's jet flap theory indicated that the method of this report yielded lift coefficients that were an average of 10.5 and 12.1 percent higher in the 30° and 60° flap angles, respectively. A comparison of three-dimensional lift coefficients with experimental data for the blown flap indicated good agreement for the 30° flap, with the predicted lift coefficient an average of 11.4 percent higher than experimental data. Calculated pressure distributions showed severe adverse pressure gradients over a large portion of the wing at angles of attack of 20° or greater.

INTRODUCTION

In recent years there has been much interest in short-takeoff-and-landing (STOL) aircraft for both civil and military applications. A STOL airplane must have the capa-

* Associate Professor of Mechanical Engineering, Michigan State University, East Lansing, Michigan.

bility for both high lift at takeoff and low drag at cruise. Past experimental work (refs. 1 to 3) demonstrated that the jet flap concept was capable of producing high lift. The jet flap airfoil injects high-velocity air over the flap surface from a slot located at the trailing edge of the airfoil, as shown in figure 1(a). (The jet flap airfoil (fig. 1(a)) is sometimes referred to as a "jet augmented flap" in the literature.) One way to implement the jet flap concept is to use an externally blown flap. This may be accomplished by using high-bypass-ratio turbofan engines which exhaust into the wing flap system.

A STOL concept under investigation at Lewis is a multiple-fan externally blown flap (fig. 1(b)). Important in this design concept is passing some of the fan exhaust through the gaps in the flaps to control the boundary layer over the wing upper surface. Some of the aerodynamic problems associated with this concept are (1) airfoil design for takeoff, cruise, and landing; (2) fan location and orientation; (3) jet penetration of propulsion system exhaust; and (4) the slot location and amount of blowing which are necessary for satisfactory boundary layer control. An analytical tool must be available to do detailed design studies of these aerodynamic problems. This tool must have the capability to handle both potential flows and boundary layers.

The potential flow analysis is the first step in obtaining an analytical tool to design STOL wing propulsion systems. By shaping the airfoil geometry, the designer can modify the wing pressure distribution to delay separation. Fan location and orientation can be improved by analysis of the pressure distributions and flow fields obtained from the potential flow solution of the combined wing and propulsion system. It is important to know the jet penetration of the propulsion system exhaust jet when considering the vertical location of the wing for a given aircraft configuration. Large penetration, under certain conditions, may cause a decrease in lift due to ground effect. Slot location and amount of blowing were not treated in this report since this would probably best be handled by boundary layer analysis (see ref. 4). From the potential flow solution, we can determine the maximum attainable lift coefficient for the wing propulsion system. Using the pressure distributions as inputs to a boundary layer program, the drag for a given engine-wing combination can be minimized.

There are many approximate potential flow theories. Some approximate methods for calculating flow over two-dimensional bodies are discussed in references 5 to 7. Most approximate methods assume, for simplification, that the body is slender or that the perturbation velocities caused by the body are small. Another type of approximate solution utilizes a distribution of singularities on or interior to the body surface. Some of these methods, based on a distribution of vorticity over the body surface are discussed in references 8 to 10. The potential flow theory that is often used when considering high-lift wing systems is Spence's flap theory, as discussed in references 11 and 12. This thin airfoil theory considers the effect of the jet sheet leaving the trailing edge of the flap, but does not take into account the effect of the propulsion system inlet and the thickness distribution of the lifting system.

The most general and comprehensive two-dimensional incompressible potential flow method and program is the Douglas method reported in references 13 to 15. This method utilizes a distribution of sources and sinks on the body surfaces, and does not require bodies to be slender nor perturbation velocities to be small. The program has the potential for dealing with distributed suction over part of the surface, and hence, can handle the propulsion system inlet airflow. However, the program cannot handle problems for which the location of part of the boundary is unknown. For a combined wing and propulsion system, the shape and location of the jet exhaust of the fan or engine is not known a priori; hence, a method is necessary to determine them.

This report presents an analysis to solve the potential flow for a STOL wing propulsion system, and the application of this analysis to a particular, externally blown flap, high-lift configuration. The analysis was accomplished by extending the two-dimensional Douglas method (ref. 14) to include the effect of suction at the propulsion system inlet, and by the development of a technique for determining the approximate location of the exhaust jet of the propulsion system. This analysis was used to obtain pressure distributions, flow fields, and lift coefficients for the externally blown flap configuration.

ANALYSIS

Representation of Wing Propulsion System

While the present development can be used for any two-dimensional configuration, it is helpful in describing the analysis to consider a particular physical system. The high-lift wing propulsion system for STOL applications under investigation at Lewis is a multiple-fan externally blown flap, as shown in figure 2(a). The wind tunnel model is semispan with a NASA 4415 airfoil section, a 66-centimeter (26-in.) chord and a 165.1-centimeter (65-in.) span. The model has eight propulsion units spaced spanwise with the inlets under the wing and the exhausts ahead of a double slotted flap. The 30° and 60° flap deflections in figure 1(b) represent typical takeoff and landing configurations.

Since the proposed STOL lifting system utilizes a large number of fans closely spaced spanwise on each wing, it is reasonable to approximate the wing section flow characteristics with a two-dimensional flow. This approximation should be valid as long as there is a sufficient number of fans for blowing to be uniformly distributed along the wing trailing edge. The representation of the two-dimensional lifting system is shown in figure 2(b). The equivalent body surface over which the potential flow is calculated consists of the airfoil with flap; the fans, which have a distributed suction at their inlet and a jet at their exit; and the jet sheet leaving the flap trailing edge.

The wing - propulsion system combination is idealized by considering it to be one solid body with suction at the fan inlet. The jet stream, as it exists from the propulsion

system is at a higher total pressure than the surrounding flow. In potential flow the total pressure is everywhere constant; hence, in this study the jet is considered to be part of the solid body. This assumes no mixing of the external free stream and the free jet. The equivalent two-dimensional-propulsion-system dimensions and jet-sheet thickness were determined from the known mass flow rate and thrust of the Lewis propulsion system (fig. 2(a)). The method used to determine the location of the free jet is discussed in a later section.

The potential flow problem for a given wing - propulsion system combination becomes one of calculating the velocities on and external to the body surface for any combination of the following variables: (1) free-stream velocity V_∞ , (2) fan or engine mass flow rate \dot{m} per unit span, (3) propulsion system thrust T per unit span, (4) flap angle θ , and (5) wing angle of attack α . The first three variables can be combined into two dimensionless parameters: the fan or engine mass flow coefficient $C_Q = \dot{m}/\rho V_\infty C$ and the thrust coefficient $C_T = T/(1/2\rho V_\infty^2 C)$. The development of the theory to handle this calculation is discussed in the following sections. (All symbols are defined in appendix A.)

Basic Equations and Boundary Conditions

The basic potential flow equation is obtained from the incompressible continuity equation together with the condition of irrotationality which gives Laplace's equation

$$\nabla^2 \varphi = 0 \quad (1)$$

where φ is the velocity potential due to the presence of the body only. To ensure uniqueness of the solution, the regularity condition at infinity is specified as

$$|\nabla \varphi|_\infty \rightarrow 0 \quad (2)$$

The velocity field \vec{V} can be expressed as the sum of the two velocities

$$\vec{V} = \vec{V}_\infty + \vec{v} \quad (3)$$

where \vec{V}_∞ is the free-stream velocity and \vec{v} is the disturbance velocity due to the presence of the body only.

A general method of solving the potential flow for an arbitrary boundary is by using a large number of sources and sinks distributed on the surface of the body. This is the

method presented in this report. The boundary condition, illustrated in figure 3, specifies that the entire normal component of velocity of the fluid at point p must be equal to the prescribed normal velocity on the surface. The contribution supplied by the source-sink distribution is $\vec{v} \cdot \vec{n}$ and that supplied by the free-stream velocity is $\vec{V}_\infty \cdot \vec{n}$. The prescribed normal velocity V_N on the surface is due to suction or blowing. Thus the boundary condition becomes

$$\vec{V}_\infty \cdot \vec{n} \Big|_p - \vec{v} \cdot \vec{n} \Big|_p = V_N \quad (4)$$

Since $\vec{v} \cdot \vec{n} = \partial\phi/\partial n$, the boundary condition on ϕ is

$$\frac{\partial\phi}{\partial n} \Big|_p = \vec{V}_\infty \cdot \vec{n} \Big|_p - V_N \quad (5)$$

Equations (1), (2), and (5) form the classic Neumann problem of potential theory, which is the basic problem we wish to solve. The direct problem, as just defined, can be solved analytically by conformal transformation only for a limited class of boundary surfaces. By using a large number of sources and sinks distributed on the surface of the body, the boundary condition can be formulated into an integral equation.

Formulation of the Boundary Condition as an Integral Equation

A simple potential function which satisfied equation (1) is the potential due to a point source. The potential at a point P due to source at q is expressed as

$$d\phi(P) = \frac{\sigma(q)ds}{r(P,q)} \quad (6)$$

where $\sigma(q)$ is the local intensity per unit area of the source and $r(P,q)$ is the distance between P and q . Because Laplace's equation is linear, the combined potential due to a distribution of sources is also a solution. By considering a continuous source distribution on the surface S , the potential at point P due to the entire body becomes

$$\phi(P) = \int_S \frac{\sigma(q)}{r(P,q)} dS \quad (7)$$

The potential as thus given satisfies equations (1) and (2), but it must also satisfy the boundary condition as given by equation (5). Applying the boundary condition requires evaluating the derivative $\partial\varphi/\partial n$ at point p on the boundary surface. The derivative of $1/r(p,q)$ becomes singular at p when p and q coincide, so that the principal value of the integral must be extracted. The principal value, according to reference 16, is $-2\pi\sigma(p)$. This is the contribution to the normal velocity at p from the source at p . The contribution of the remainder of the sources to the normal velocity is given by the derivative of the integral of equation (7) evaluated on the boundary. The normal derivative of φ becomes

$$\left. \frac{\partial\varphi}{\partial n} \right|_p = -2\pi\sigma(p) + \int_S \frac{\partial}{\partial n} \left[\frac{1}{r(p,q)} \right] \sigma(q) \, dS \quad (8)$$

Applying the condition of equation (5) to equation (8) results in the integral equation for the source-intensity distribution $\sigma(p)$

$$2\pi\sigma(p) - \int_S \frac{\partial}{\partial n} \left[\frac{1}{r(p,q)} \right] \sigma(q) \, dS = -\vec{V}_\infty \cdot \vec{n} + V_N \quad (9)$$

This equation is a Fredholm integral equation of the second kind whose solution is the central problem of the analysis.

The quantity $-\partial/\partial n [1/r(p,q)]$ is called the kernel of the integral equation and depends only on the geometry of the surface. The first term of equation (9) is the normal velocity induced at p by a source at p . The second term is the combined effect of the sources at other points q on the surface of the body. The specific boundary conditions determine the right side of equation (9). The first term on the right is the normal component of the free-stream velocity at p . The second term on the right is the prescribed normal velocity on the boundary surface at p . The solution of this Fredholm integral equation then requires determining the unknown function σ on the body surface.

Solution of Integral Equation

Since the boundary of the wing propulsion system is completely arbitrary, the integration of equation (9) with respect to S should be done numerically. The boundary is

approximated by a large number of surface elements whose characteristic lengths are small compared to the body. It is assumed that the surface element is a flat segment, as shown in figure 4. As the number of elements increases, the assumed model approaches the shape of the body. The value of the source intensity is assumed to be constant over each surface element. By assuming this constant intensity over each element, the problem becomes one of finding a finite number of values of σ , one for each of the surface elements. This gives a number of linear equations equal to the number of unknown values of σ . On each element a control point (the midpoint of the element) is selected where equation (8) is required to hold. Rewriting equation (8) in summation form yields

$$\left. \frac{\partial \varphi}{\partial n} \right|_{\mathbf{p}} = -2\pi\sigma(\mathbf{p}) + \sum_{\mathbf{p} \neq \mathbf{q}} \frac{\partial}{\partial n} \left[\frac{1}{r(\mathbf{p}, \mathbf{q})} \right] \sigma(\mathbf{q}) \Delta S \quad (10)$$

The right side of equation (10) now becomes a matrix consisting of the normal velocities induced by a source of intensity σ at the control points of all elements. The normal velocity at the control point of the i^{th} element due to all surface elements is denoted as

$$\left. \frac{\partial \varphi}{\partial n} \right|_{\mathbf{i}} = A_{ii}\sigma_i + \sum_{\substack{j=1 \\ j \neq i}}^N A_{ij}\sigma_j = \sum_{j=1}^N A_{ij}\sigma_j \quad (11)$$

Thus

$$A_{ij} = \frac{\partial}{\partial n} \left[\frac{1}{r(\mathbf{p}, \mathbf{q})} \right] \Delta S$$

where i corresponds to \mathbf{p} and j corresponds to \mathbf{q} .

The source densities of all the surface elements must be determined in such a way that the normal velocity condition is satisfied at all control points. This results in

$$\sum_{j=1}^N A_{ij}\sigma_j = -\vec{V}_{\infty} \cdot \vec{n}_i + V_{N,i} \quad (12)$$

This set of linear algebraic equations is an approximation to the integral equation (9).

Both $\vec{V}_\infty \cdot \vec{n}$ and the prescribed normal velocity V_N , in general, vary over the body surface. The linear equations are solved by a procedure of successive orthogonalization, as discussed in reference 17. Once the linear equations have been solved, flow velocities may be calculated for points on and off the body surface. The method just described is used to obtain the basic solutions of potential flow.

Basic Solutions

The superposition of any solutions to the integral equation (9) is also a solution since Laplace's equation is linear. Hence, the flow about a body may be thought of as a linear combination of four basic flows illustrated in figure 5:

- (1) Uniform flow at zero angle of attack
- (2) Uniform flow at 90° angle of attack
- (3) Vortex flow
- (4) Flow due to suction or blowing

Uniform flow solutions. - The uniform flow solutions are solutions due to free-stream velocity (rectilinear flow) past the body surface at 0° and 90° , respectively. For these basic solutions, the boundary condition of zero normal velocity on the surface must be satisfied. Then the prescribed velocity normal to the surface must be zero for the basic uniform flow solutions. From equation (5) the boundary condition becomes

$$\left. \frac{\partial \phi}{\partial n} \right|_p = \vec{V}_\infty \cdot \vec{n} \Big|_p \quad (13)$$

The solution for the body at any angle of attack may be obtained by a linear combination of the 0° and 90° uniform flow solutions.

Vortex flow solution. - For a lifting body the circulation is obtained by placing a vortex at any convenient location within the body. The boundary condition of zero normal velocity on the surface still applies (eq. (5)) except that now \vec{V}_∞ is replaced by the vortex velocity at any point. If \vec{V}_v represents the velocity at any point p on the body caused by the vortex, the boundary condition for the basic vortex solution becomes

$$\left. \frac{\partial \phi}{\partial n} \right|_p = \vec{V}_v \cdot \vec{n} \Big|_p \quad (14)$$

Suction flow solution. - The suction flow solution is obtained by specifying a prescribed normal velocity V_N on the surface of the body with a zero free-stream velocity. From equation (5) the boundary condition for the basic suction velocity solution becomes

$$\left. \frac{\partial \phi}{\partial n} \right|_p = -V_N \quad (15)$$

For each basic solution, the velocities on the body surface and at prescribed locations in the flow field may be obtained. From the basic solutions the total combined solution may be obtained.

Combination Solution

The total velocity tangent to the body surface can be obtained by adding the tangential velocities of the four basic solutions.

$$V_t = V_{t,0} \cos \alpha + V_{t,90} \sin \alpha + \Gamma V_{t,v} + V_{t,s} \quad (16)$$

where α is the angle of attack.

The circulation Γ is determined by satisfying the Kutta condition at the trailing edge of the body. This condition stipulates that the flow at the body trailing edge be smooth. Thus, the tangential velocities above and below the trailing edge must be equal in magnitude. If ΔV is defined as $\Delta V = V_{\text{upper}} - V_{\text{lower}}$, the Kutta condition is satisfied if $\Delta V = 0$ at the body trailing edge. Then from equation (16)

$$\Delta V_{t,0} \cos \alpha + \Delta V_{t,90} \sin \alpha + \Delta V_{t,s} + \Gamma \Delta V_{t,v} = 0 \quad (17)$$

Solving for Γ yields

$$\Gamma = - \frac{\Delta V_{t,0} \cos \alpha + \Delta V_{t,90} \sin \alpha + \Delta V_{t,s}}{\Delta V_{t,v}} \quad (18)$$

Once the combined velocities on the body surface are known, the pressure coefficient, the lift coefficient, and the thrust coefficient can be obtained (see appendix B).

For off-body points it is more convenient to combine the basic source intensities rather than the basic velocities. The equation for the combined source intensity is

$$\sigma = \sigma_0 \cos \alpha + \sigma_{90} \sin \alpha + \Gamma \sigma_v + \sigma_s \quad (19)$$

Then, the x and y components of velocity are calculated from the combined source in-

tensities. This approach is the same as that used in reference 15, with the addition of the basic suction source intensity being added to the other basic source intensities.

Location of Propulsion System Exhaust Jet

The location of the propulsion system exhaust jet is determined by the following variables: (1) jet angle at flap trailing edge θ , (2) jet penetration H , (3) jet angle at trailing edge of jet θ_1 , and (4) total length of the free jet L_T . The representation of these variables is shown in figure 2(b). It was assumed that the free jet leaves the flap trailing edge at the flap angle θ . The flap angle is defined as the angle between the free-stream direction and lower flap surface. After the jet leaves the trailing edge, the free-stream velocity turns the jet, which approaches a horizontal asymptote at several chord lengths beyond the airfoil leading edge. For typical thrust coefficients C_T corresponding to takeoff and landing conditions, this occurs at approximately four chord lengths from the airfoil leading edge (see ref. 10).

For a reasonable approximation to the jet shape, the lift coefficient is expected to depend principally on the vertical location of the jet asymptote. The problem then becomes one of finding the jet penetration H as shown in figure 2(b). Initially, the penetration was assumed and a cubic equation used to approximate the shape of the jet sheet. A cubic equation is the simplest expression that adequately approximates the jet shapes obtained from Spence's jet flap theory of reference 12. The correct distance H is that value for which the vertical component of thrust at the flap trailing edge balances the integrated vertical pressure forces on the free jet. Several values of H were assumed until the correct value of H was obtained.

Since the angle of the free jet is not exactly horizontal several chord lengths beyond the wing, a small angle θ_1 (5° or less) was assumed. The length of the jet L_T was extended until the vertical component of force on the end of the jet (last 5 percent of the jet) was negligible for the chosen angle θ_1 . Thus, if the jet is extended beyond this length, it gives no significant contribution to the lift coefficient. Neglecting the vertical component of thrust at the end of the jet for an angle of 5° results in only a 3-percent variation in lift coefficient. Since the body representing the wing, flap, and jet is considered a lifting body, it was assumed to be closed at the jet trailing edge and the Kutta condition was applied here.

Inlet Air Suction

The inlet air suction was obtained by prescribing the velocity profile at the fan face.

From the prescribed normal velocity V_N on the surface of the body, the basic suction solution is obtained. This gives the desired mass flow rate for the inlet of the propulsion system.

DISCUSSION

Validity of Analysis

Inlet air suction. - To help ensure validity of the analysis, comparisons were made with known existing flow solutions. One existing solution solves the suction problem indirectly. It is also based on the Douglas method, but has application only to inlets and ducts (see ref. 18). This method utilizes three basic solutions, shown in figure 6, to obtain a combined solution of physical interest. The flow about the inlet is obtained by considering the three basic solutions: \bar{V}_1 with inlet duct extension closed, \bar{V}_2 with the duct open, and \bar{V}_3 the crossflow solution. With these three solutions any combination of free-stream velocity and mass flow through the inlet can be obtained. The duct must be extended far downstream of the region of interest to obtain valid solutions. This method could not be used to get solutions for a wing-engine combination since the body must be closed to consider it a lifting body. To make a comparison between this existing flow solution and the method presented in this report a two-dimensional inlet, shown in figure 7, was considered. This inlet was chosen because experimental data were available. In the present analysis, mass flow through the inlet was obtained by considering a distributed suction V_N downstream of the inlet (see fig. 7). Comparison of the nondimensional surface velocities for the two methods are shown in figures 8(a) and (b). Also shown is experimental data obtained from reference 19. The reference velocity V_{ref} was arbitrarily selected as the average velocity at an x/L of 0.89. Agreement between the two predictions is excellent for both the surface and centerline velocities. Comparison of experimental data with the prediction is quite acceptable for the centerline velocities. There is a slight variation between the experimental and predicted surface velocities. One reason for this variation could be boundary layer effects. The preceding discussion indicates that the combined uniform flow and suction solution is valid.

Exhaust jet shape. - For a valid solution of a wing propulsion system there must be a reasonable approximation to the jet shape. The lift coefficients and pressure distributions for a given thrust coefficient depend principally on the flap angle θ and jet penetration H , as outlined in the section Location of Propulsion System Exhaust Jet, and not on the precise local shape of the jet. This is illustrated in figure 9, which considers various free jet shapes for a 30° flap. For clarity the jet thickness is not shown. The assumed cubic equation is shown, along with representative upper and lower bounds for

the jet shape. For the jet shapes A and C shown, the solution results in only a ± 2.5 percent variation in lift coefficient from the assumed cubic shape B. This percent variation is distributed over the entire wing surface, as illustrated by the pressure distributions in figure 9(b). Figure 9(b) shows only a 3-percent variation in pressure distribution for the jet shapes considered. Thus, the lift coefficients and pressure distributions depend principally on the flap angle and jet penetration and not on the precise local shape of the jet for the present configuration.

As a point of interest, a comparison of the jet shape based on the Spence's theory of reference 12 was made with the jet shape obtained from the present method. Reference 12 assumes that all flow deflections from the free stream are not large and vortex distributions are placed on the x-axis rather than on the airfoil or jet. Thus, a comparison could only be made for relatively small flap deflections (30° or less). A comparison of the nondimensional jet shape predicted from Spence's theory and from the method of this report is shown in figure 10 for a 30° flap deflection and a thrust coefficient of 3. The basic shapes of the two cases are the same close to the wing. The jet penetration of the present method is larger than Spence's theory at the greater distances, as would be expected. The present method, besides not assuming small angle approximations, includes the wing thickness and camber effect which would increase the lift coefficient and would also result in a greater penetration.

Example Applications

Flow field. - Potential flow solutions are adequate representations of the flow around bodies if the surface boundary layers are thin and remain attached. It is assumed that the final design of a high-lift wing propulsion system will be one in which boundary layer separation is prevented at relatively high angles of attack and flap settings. Representative flow fields for an externally blown flap, high-lift configuration are shown in figures 11(a) to (c). The flow fields were obtained by sketching streamlines tangent to the calculated velocity vectors at various points in the flow. The wing propulsion system is shown, along with the shape of the jet exhaust of the propulsion system. For the conditions shown, the upwash angles at the propulsion system inlet are quite large, varying from 60° to 90° depending on flap angles and wing angles of attack. Two stagnation points occur on the lifting body. One occurs ahead of the inlet below the leading edge of the wing, and the other occurs downstream of the inlet on the under surface of the fan. Both stagnation points move further aft as the flap angle and the wing angle are increased. By observation of the flow fields it is seen that the under surface of the wing is in a relatively stagnant region. The jet penetration increases with angle of attack (figs. 11(a) and (b)). For a flap angle of 60° (fig. 11(c)) the jet penetration distance is approximately

three chord lengths at five chord lengths beyond the wing leading edge. This jet penetration is important when considering the effect of the ground on lift coefficient.

Pressure distribution. - The predicted pressures on the surface of the airfoil are valid only if the boundary layer is very thin and attached to the surface. The potential flow pressure distributions can be used both to calculate the boundary layer growth on the surface of the airfoil and as a design aid for the combined wing and propulsion system. Pressure distributions on the wing upper surface with a 30° blown flap at various angles of attack are presented in figure 12. The incompressible pressure coefficient, corresponding to the minimum pressure point, ranges from -7.5 to -51 for the 0° and 20° angle of attack, respectively. For the high negative pressure coefficients, compressibility effects should be taken into account. The compressible pressure distributions can be obtained by making standard compressibility corrections to the incompressible pressure distributions (ref. 20). These extremely high negative pressure coefficients correspond to the very high lift coefficients which are discussed in the following section. The minimum pressure point for all angles of attack occurs very near the leading edge of the airfoil, and severe adverse pressure gradients over a large portion of the wing result at the higher angles of attack. The stagnation point moves further under the leading edge as angle of attack increases, resulting in high velocity gradients about the leading edge.

To illustrate the effect of the inlet airflow of the propulsion system and the effect of the exhaust jet a comparison was made of the pressure distributions for (1) the wing alone, (2) the wing with jet but without inlet air suction, and (3) the wing with inlet air suction and jet. This comparison is presented in figure 13 for a 30° flap. At the minimum pressure point for the wing alone there exists a pressure coefficient of -4.8 near the wing leading edge, followed by a mild adverse pressure gradient. The wing with jet but without inlet air suction would be representative of a jet flap airfoil shown in figure 1(a). Jet flap theory does not include the effect of the inlet airflow of the propulsion system. For the wing with jet (without suction) the pressure coefficient is about -18 at the minimum pressure point, and there is a severe adverse pressure gradient over a large portion of the wing upper surface. When the effect of the suction at the propulsion system inlet is included, the magnitude of the pressures is reduced considerably over the wing upper surface, resulting in a minimum pressure coefficient of -7.6, followed by a much milder adverse pressure gradient. It may appear from the upper-surface pressure distributions of figure 13 that the lift with the jet alone is much larger than the lift associated with the jet with suction; but this is not the case if both upper and lower surfaces of the airfoil are considered. The change in pressure distribution between the zero suction case and the suction case is a result of a shift in the stagnation point ($C_p = 1.0$) on the under surface of the wing. For the wing without suction, one stagnation point occurs just ahead of the inlet of the propulsion system. For the wing with suction, this stagnation point moves closer to the wing leading edge and another stagnation point occurs on the under surface of the fan (fig. 11(a)). The corresponding shift in the pressure distributions on both the

upper and lower surfaces presented in figure 13 results in less than 5 percent decrease in lift when the effect of inlet suction is included for the selected inlet location. The preceding discussion indicates that the effect of suction resulting from a fan or inlet installed under the wing affects the pressure distribution on the wing upper surface favorably, with only a small effect on total lift coefficient.

Lift coefficients. - In order to further indicate the applicability of the present analysis a comparison (fig. 14) was made between Spence's theory (ref. 12) and the method of this report for two-dimensional lift coefficients for the blown flap configuration (fig. 1(b)). The lift coefficients predicted by the method of this report for the 30° flap range from 6.5 to 13, while those for the 60° flap range from 15 to 21. The lift coefficients predicted by the present method generally range from 9.1 to 12 percent and from 10.6 to 13.6 percent higher than Spence's theory for the 30° and 60° flap, respectively. This difference exists since Spence's theory does not take into account the effects of the thickness and camber of the wing. The suction effect decreases the lift by approximately 5 percent, as discussed previously. The thickness and camber effect corresponds to approximately 15 percent increase in lift coefficient.

The two-dimensional lift coefficients were used to determine three-dimensional lift coefficients to compare with experimental data of a semispan blown flap model (fig. 2(a)). The three-dimensional lift coefficient is

$$C_L = fC_l \quad (20)$$

where f is a function of aspect ratio and thrust coefficient (assuming an elliptical lift distribution) and was obtained from reference 21 as

$$f = \frac{AR + \frac{2C_T}{\pi}}{AR + 2 + 0.604(C_T)^{1/2} + 0.876C_T} \quad (21)$$

Calculated three-dimensional lift coefficients along with experimental data obtained from the Lewis test program are presented in figure 15. The aspect ratio was 5 for the blown flap model. The lift coefficients predicted by the method of this report range from 4 to 7.5 and from 9 to 13 for the 30° and 60° flap, respectively. The lift coefficients predicted by the method of this report for the 30° flap (fig. 15(a)) range from 10.8 to 12 percent higher than the experimental data. There is good agreement between Spence's theory and experiment for the 30° flap case. The lift coefficients predicted by the method of this report for the 60° flap (fig. 15(b)) range from 28.6 to 28.4 percent greater

than the experimental data, while those predicted by Spence's theory range from 13.5 to 18.1 percent greater than the data.

The lift coefficient calculated from potential theory is the maximum attainable lift coefficient for each configuration corresponding to complete boundary layer control and negligible viscous effects. Thus, it is expected that the predicted lift coefficients be greater than the experimental data. The large variation in lift coefficients between theory and experiment for the 60° flap configuration may indicate that this configuration did not have optimum boundary layer control and that improvements could be made in obtaining better experimental coefficients.

CONCLUDING REMARKS

A method was developed to determine the two-dimensional potential flow solution of STOL wing propulsion systems. The Douglas potential flow analysis was extended to include the effect of suction at the propulsion system inlet and to provide a technique for determining the approximate location of the exhaust jet of the propulsion system. The effect of suction was obtained by combining the Douglas basic suction solution with the uniform flow solution for a lifting body. The jet exhaust was considered as part of the solid body and its location was determined by balancing the vertical component of thrust at the flap with the integrated vertical pressure forces on the free jet.

The applicability of the program is illustrated by considering a multiple-fan externally blown flap under high-lift conditions. The results indicated high upwash angles at the fan inlet and large jet penetration at high angles of attack. The predicted two-dimensional lift coefficients for a 30° flap were an average of 10.5 percent higher than predicted by Spence's jet flap theory which neglects thickness effects. The predicted three-dimensional lift coefficients were an average of 11.4 percent higher than experimental data for the 30° blown flap high-lift configuration. The calculated pressure distributions indicated that the minimum pressure point is near the leading edge (less than 2 percent of chord) of the airfoil, with severe adverse pressure gradients at high angles of attack.

The ability of the potential flow solution to predict pressure distributions, lift coefficients, and flow fields makes it extremely useful as a tool in the analysis and design of a STOL wing propulsion system. The pressure distributions obtained from the potential flow solution can be used to determine the boundary layer growth and separation on the airfoil of the wing propulsion system. These distributions can be used to design the airfoil and to determine the optimum location and orientation of the propulsion system. From the predicted pressure distributions and boundary layer calculations, the frictional drag can be obtained for a given wing propulsion system. The potential flow solution can

be used to determine the jet penetration - an important quantity when considering ground effect.

The analysis has application not only to wing propulsion systems, but to any lifting or nonlifting body where suction or blowing is applied.

Lewis Research Center,

National Aeronautics and Space Administration,

Cleveland, Ohio, April 7, 1971,

721-03.

APPENDIX A

SYMBOLS

A_{ii}	normal velocity of element i caused by a unit source at element i
A_{ij}	normal velocity of element i caused by a unit source at element j
AR	aspect ratio
C	chord length
C_L	three-dimensional lift coefficient
C_l	two-dimensional lift coefficient
C_p	pressure coefficient
C_Q	mass flow coefficient
C_T	thrust coefficient
F_y	force in vertical direction
f	correction factor (eq. (21))
H	jet penetration (fig. 2(b))
L	length
L_T	total length of free jet
M	number of elements that describe the jet
\dot{m}	fan or engine mass flow rate per unit span
N	number of elements that describe the body
n	a normal to the body surface
P^*	arbitrary point in the flow field off the surface
p	static pressure
r	distance between two points
S	surface of body
T	thrust per unit span
V	velocity
v	disturbance velocity
x	Cartesian coordinate
y	Cartesian coordinate

α angle of attack
 α_i orientation of surface element
 Γ nondimensional circulation
 η turning efficiency of exhaust jet
 θ flap angle (fig. 2(b))
 θ_1 jet angle at trailing edge of jet (fig. 2(b))
 σ surface source intensity per unit area
 ρ density
 φ velocity potential

Subscripts:

i control point of i^{th} element
 j control point of j^{th} element
 N normal
 p arbitrary point on the surface
 q a surface point
 ref reference
 s suction flow solution
 t tangential
 v vortex flow solution
 ∞ free stream
 0 flow solution at zero angle of attack
 90 flow solution at 90° angle of attack

Superscript:

\rightarrow vector

APPENDIX B

CALCULATION OF FLOW QUANTITIES

Once the combined velocities on the body surface are calculated, the pressure distribution and the lift coefficient of the body can be found. The equation of motion for steady, incompressible, inviscid fluid can be expressed as

$$(\vec{\nabla} \cdot \nabla) \vec{V} = -\frac{1}{\rho} \nabla p \quad (\text{B1})$$

For potential (irrotational) flow, Bernoulli's equation results

$$\frac{p}{\rho} + \frac{1}{2} V^2 = \text{Constant} \quad (\text{B2})$$

The pressure coefficient C_p is defined as

$$C_p = \frac{p - p_\infty}{\frac{1}{2} \rho V_\infty^2} \quad (\text{B3})$$

By use of equation (B2)

$$C_p = 1 - \frac{V^2}{V_\infty^2} \quad (\text{B4})$$

The two-dimensional lift coefficient is defined as

$$C_l = \frac{L}{\frac{1}{2} \rho V_\infty^2 C} \quad (\text{B5})$$

This can be obtained by integration of the pressure distribution over the surface of the body. Since $L = \int_S p_i \cos \alpha_i dS_i$,

$$C_l = \frac{1}{C} \sum_{i=1}^N C_{p,i} \cos \alpha_i \Delta S_i \quad (\text{B6})$$

where $C_{p,i}$ represents the pressure coefficient at the control point of the i^{th} element. The thrust coefficient is defined as

$$C_T = \frac{T}{\frac{1}{2} \rho V_\infty^2 C} \quad (\text{B7})$$

where T is the exit thrust of the propulsion system. The exit thrust is obtained from the vertical force on the jet, the jet deflection angle, and the experimental turning efficiency η between the propulsion system exhaust and the trailing edge of the flap. Then

$$T = \frac{F_y}{(\sin \theta)(\eta)} \quad (\text{B8})$$

where η is the turning efficiency of the exhaust jet. The vertical force is calculated by integration of the pressures on the jet

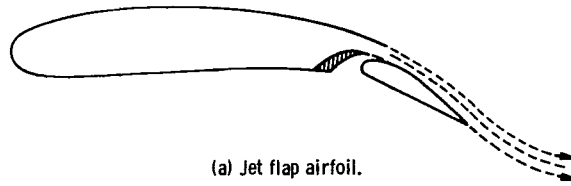
$$F_y = \sum_{i=1}^M p_i \cos \alpha_i \Delta S_i \quad (\text{B9})$$

where α_i is the angular orientation of the i^{th} element.

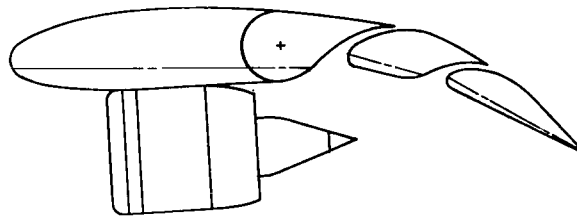
REFERENCES

1. Koenig, David G.; Corsiglia, Victor R.; and Morelli, Joseph P.: Aerodynamic Characteristics of a Large-Scale Model with an Unswept Wing and Augmented Jet Flap. NASA TN D-4610, 1968.
2. Campbell, John P.; and Johnson, Joseph L., Jr.: Wind-Tunnel Investigation of an External-Flow Jet-Augmented Slotted Flap Suitable for Application to Airplanes with Pod-Mounted Jet Engines. NACA TN 3898, 1956.
3. Parlett, Lysle P.; Freeman, Delma C., Jr.; and Smith, Charles C., Jr.: Wind-Tunnel Investigation of a Jet Transport Airplane Configuration with High Thrust-Weight Ratio and an External-Flow Jet Flap. NASA TN D-6058, 1970.
4. Gartshore, I. S.: Predictions of the Blowing Required to Suppress Separation from High-Lift Aerofoils. Paper 70-872, AIAA, July 1970.
5. Thwaites, Bryan, ed.: Incompressible Aerodynamics. Clarendon Press, Oxford, 1960.
6. Weber, J.: The Calculation of the Pressure Distribution over the Surface of Two-Dimensional and Swept Wings with Symmetrical Aerofoil Sections. Rep. R&M 2918, Aeronautical Research Council, Gt. Britain, 1956.
7. Goldstein, S.: Approximate Two-Dimensional Aerofoil Theory. Part II. Velocity Distributions for Cambered Aerofoils. Rep. CP-69, Aeronautical Research Council, Gt. Britain, 1952.
8. Anon.: A Direct Iteration Method for the Calculation of the Velocity Distribution of Bodies of Revolution and Symmetrical Profiles. Rep. ARL/RI/G/HY/12/2, Admiralty Research Laboratory, Gt. Britain, Aug. 1951.
9. Jacob, K.: Some Programs for Incompressible Aerodynamic Flow Calculations. Tech. Rep. 122, California Inst. Techn. Computing Center, 1960.
10. Davenport, F. J.: Singularity Solutions to General Potential-Flow Airfoil Problems. Rep. D6-7202, Rev., Boeing Co., 1963.
11. Spence, D. A.: The Lift Coefficient of a Thin, Jet-Flapped Wing. Proc. Roy. Soc. (London), Ser. A, vol. 238, Dec. 4, 1956, pp. 46-68.
12. Spence, D. A.: The Lift on a Thin Aerofoil with a Jet-Augmented Flap. Aeron. Quart., vol. 9, Aug. 1958, pp. 287-299.
13. Smith, A. M. O.; and Pierce, J.: Exact Solution of the Neumann Problem. Calculation of Noncirculatory Plane and Axially Symmetric Flows about or Within Arbitrary Boundaries. Rep. ES-26988-V, Douglas Aircraft Co., Apr. 25, 1968.

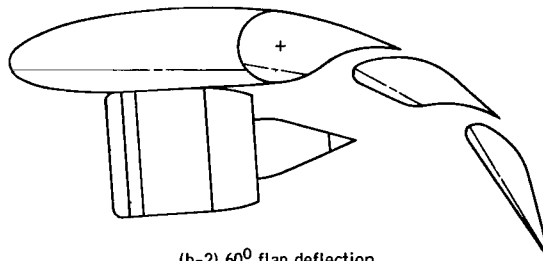
14. Giesing, Joseph P.: Extension of the Douglas Neumann Program to Problems of Lifting Infinite Cascades. Rep. LB-31653, Douglas Aircraft Co., July 2, 1964. (Available from DDC as AD-605207.)
15. Giesing, Joseph P.: Potential Flow About Two-Dimensional Airfoils. Part I: A Summary of Two-Dimensional Airfoil Methods. Part II: Solution of the Flow Field About One or More Airfoils of Arbitrary Shape in Uniform or Nonuniform Flows by the Douglas Neumann Method. Rep. LB-31946, Douglas Aircraft Co., Dec. 1, 1965.
16. Kellogg, Oliver D.: Foundations of Potential Theory. Dover Publ., Inc., 1953.
17. Purcell, Everett W.: The Vector Method of Solving Simultaneous Linear Equations. J. Math. Phys., vol. 32, 1953, pp. 180-183.
18. Stockman, Norbert O.: Potential Flow Solutions for Inlets of VTOL Lift Fans and Engines. Analytic Methods in Aircraft Aerodynamics. NASA SP-228, 1970, pp. 659-681.
19. Emslie, K.: Wind Tunnel Test on Models of V.T.O. Aircraft. Aircraft Eng., vol. 38, no. 6, June 1966, pp. 8-13.
20. Shapiro, Ascher H.: The Dynamics and Thermodynamics of Compressible Fluid Flow. Vol. I. Ronald Press, 1953.
21. Williams, J.; Butler, F. J.; and Wood, M. N.: The Aerodynamics of Jet Flaps. Rep. R&M 3304, Aeronautical Research Council, Gt. Britain, 1963.



(a) Jet flap airfoil.



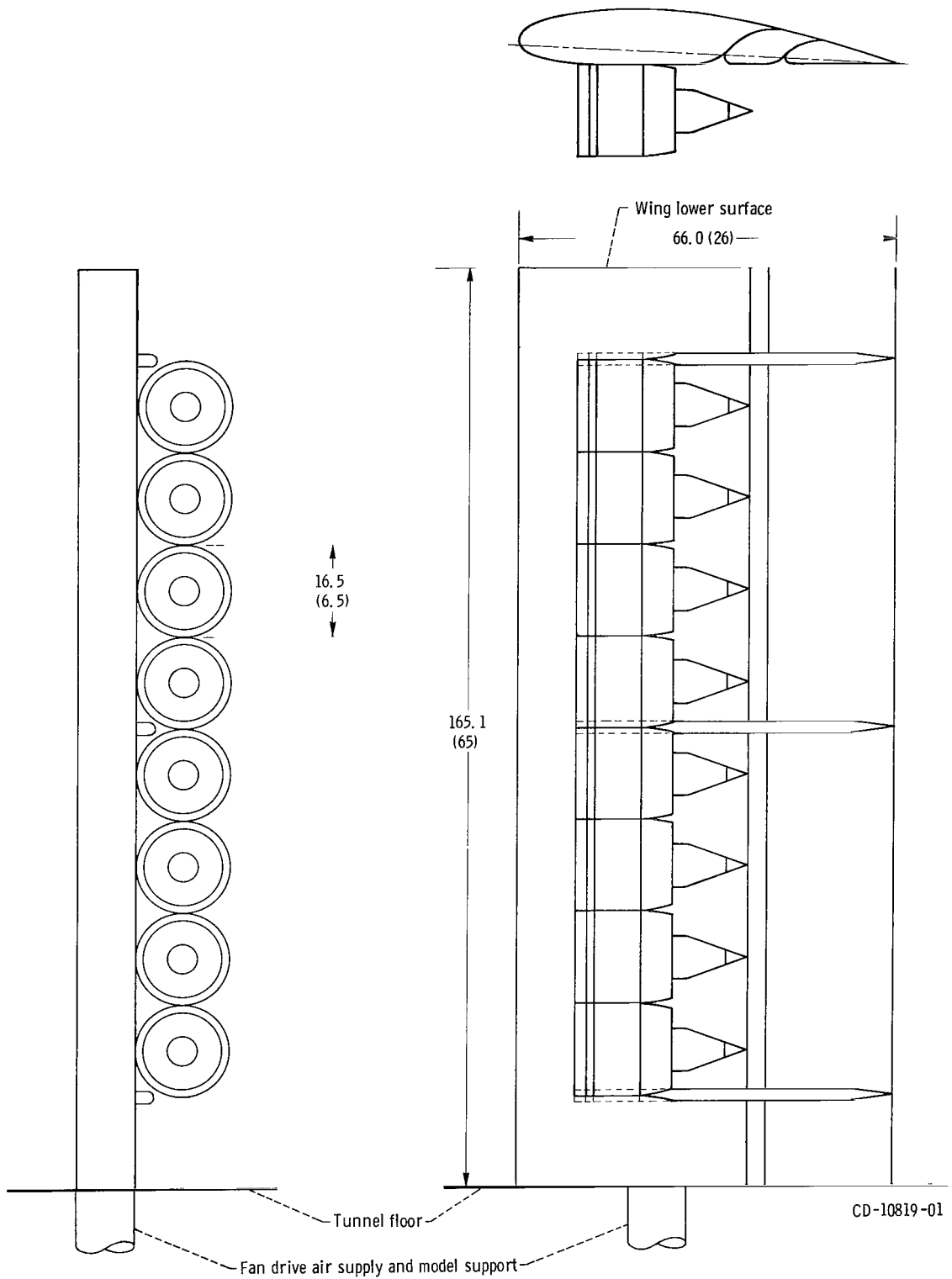
(b-1) 30° flap deflection.



(b-2) 60° flap deflection.

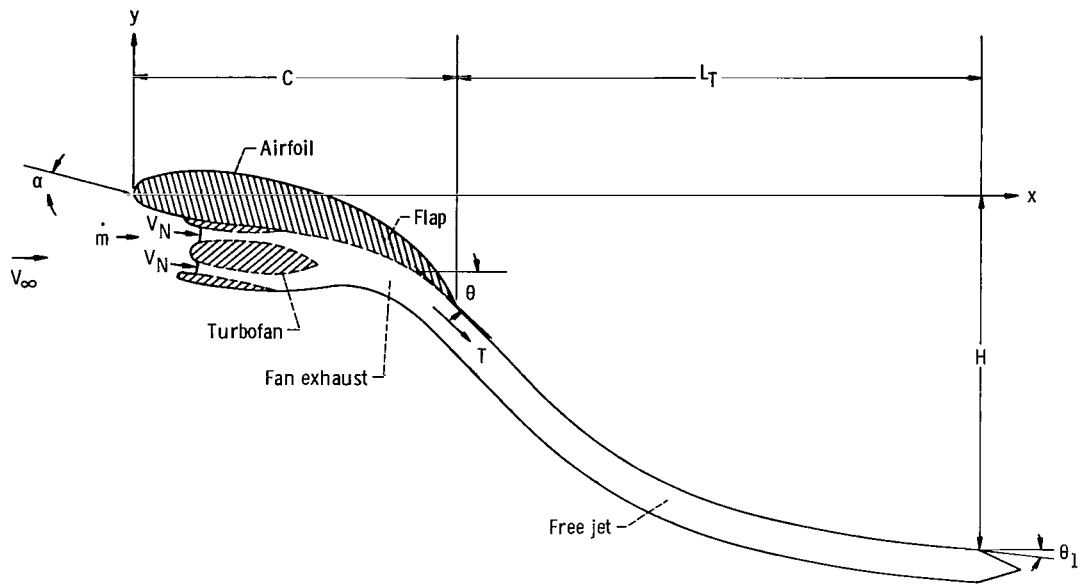
(b) Externally blown flap wing section.

Figure 1. - Types of wing flap systems considered.



(a) Schematic of model. (Dimensions are in cm (in.).)

Figure 2. - Lewis wind tunnel model of multiple-fan, blown flap, wing propulsion system.



(b) Two-dimensional representation of wing propulsion system.

Figure 2. - Concluded.

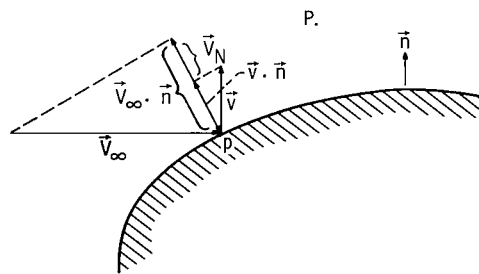


Figure 3. - Representation of boundary condition on body surface.

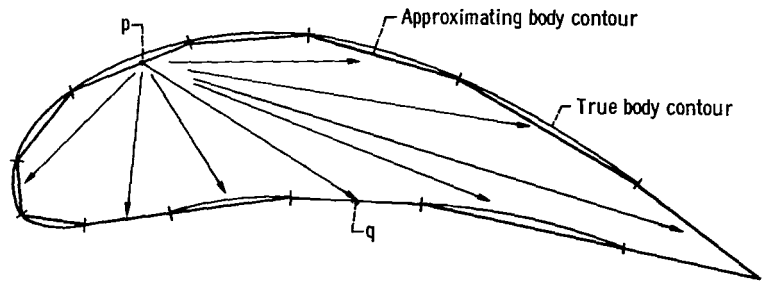


Figure 4. - Finite-element approximation to body surface.

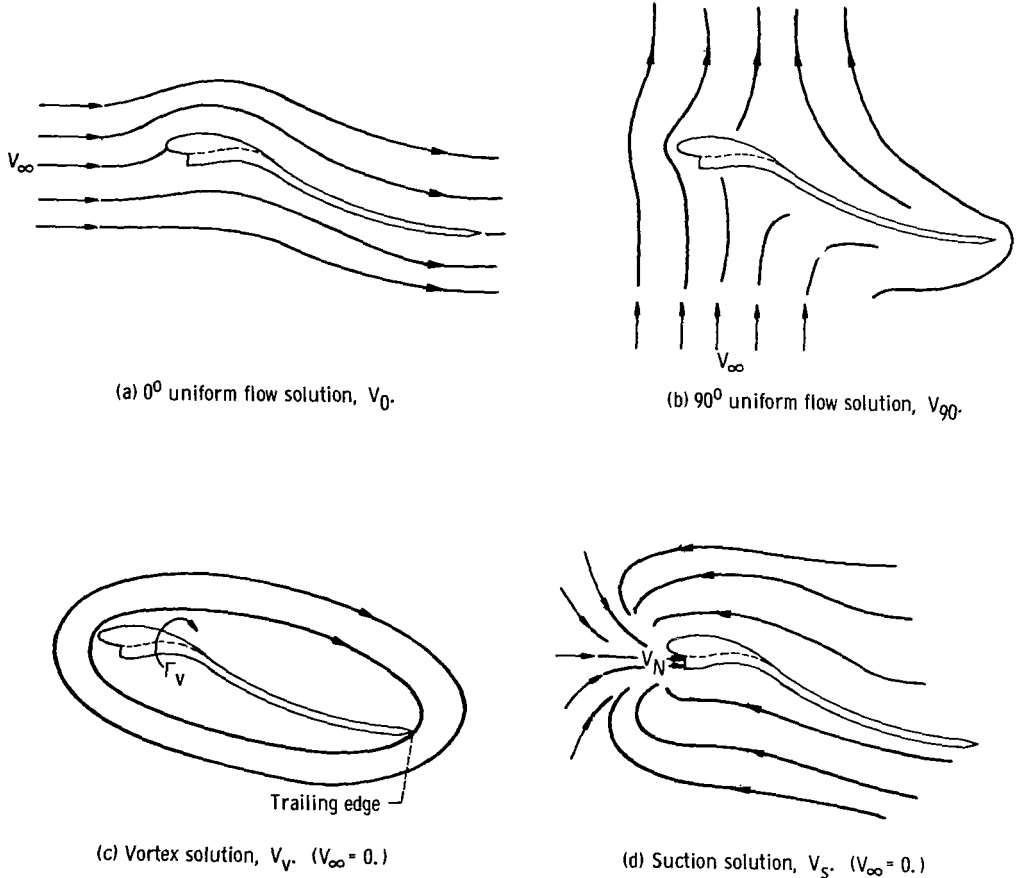


Figure 5. - Basic solutions of potential flow.

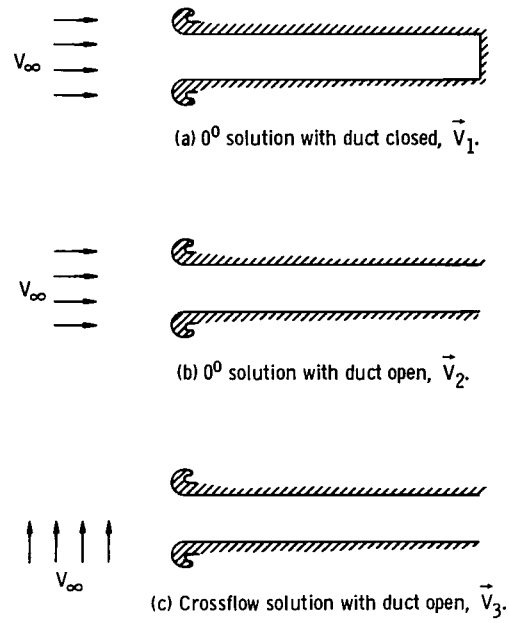


Figure 6. - Basic solutions for inlet.

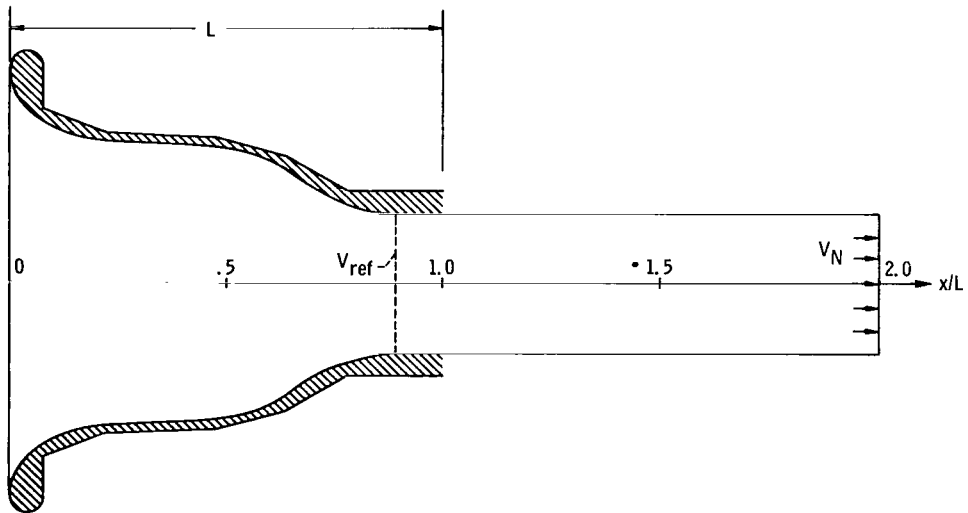


Figure 7. - Two-dimensional inlet configuration.

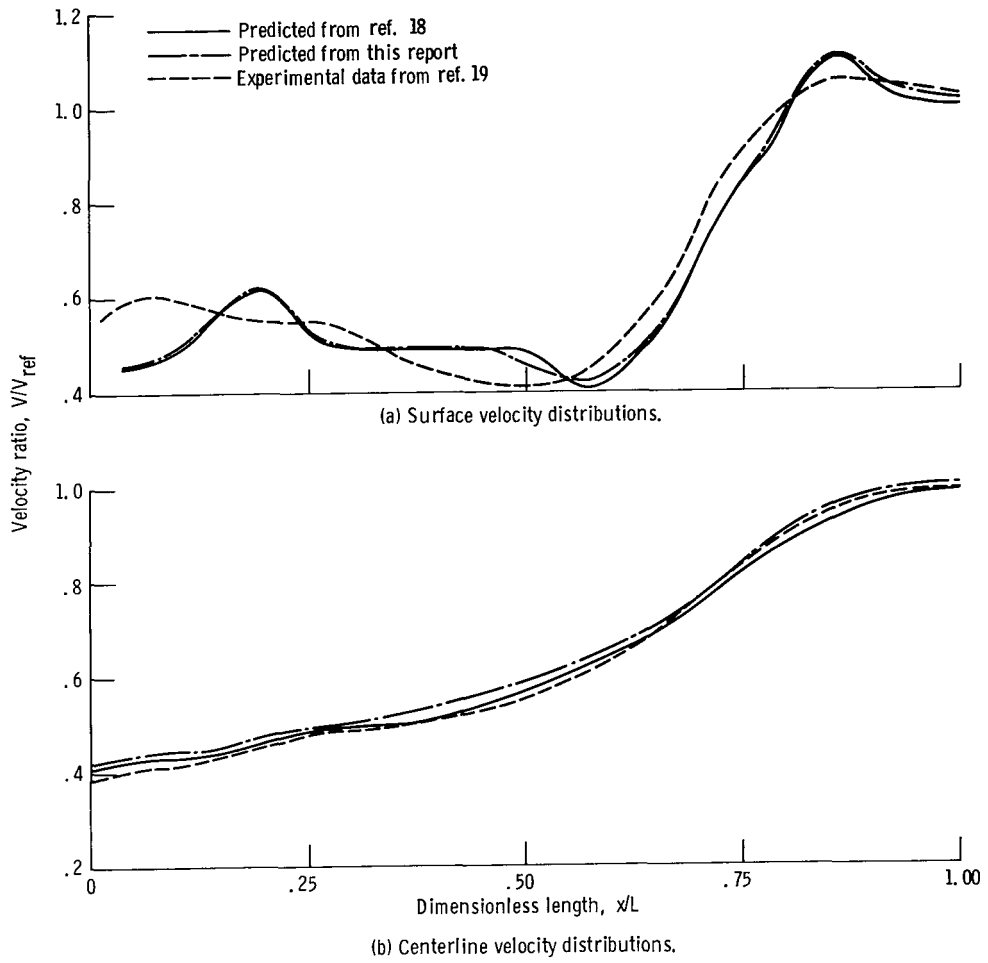
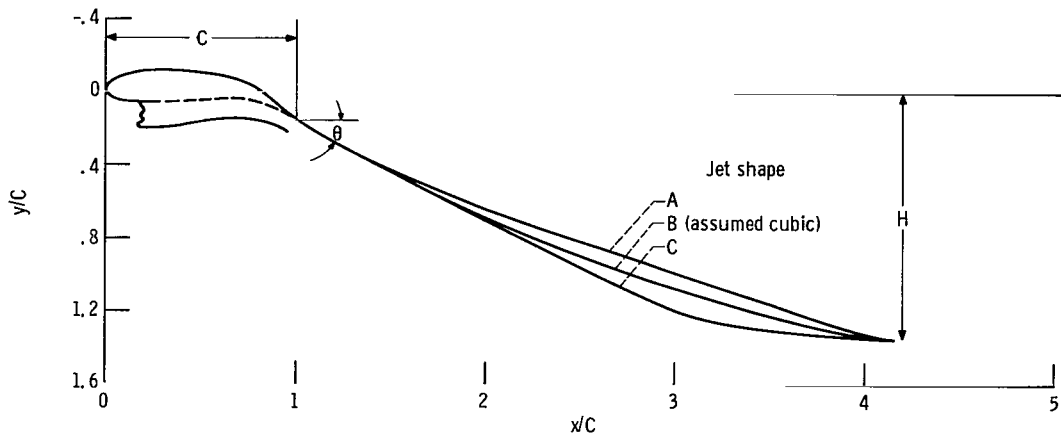
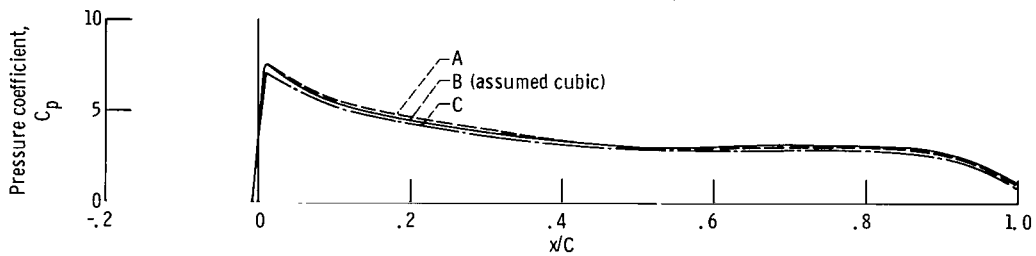


Figure 8. - Comparison of theoretical velocity distributions with experimental data for two-dimensional inlet.



(a) Illustration of jet shapes.



(b) Upper-surface pressure distributions.

Figure 9. - Effect of jet shapes on upper-surface pressure distribution. Flap angle, 30° ; wing angle of attack, 0° .

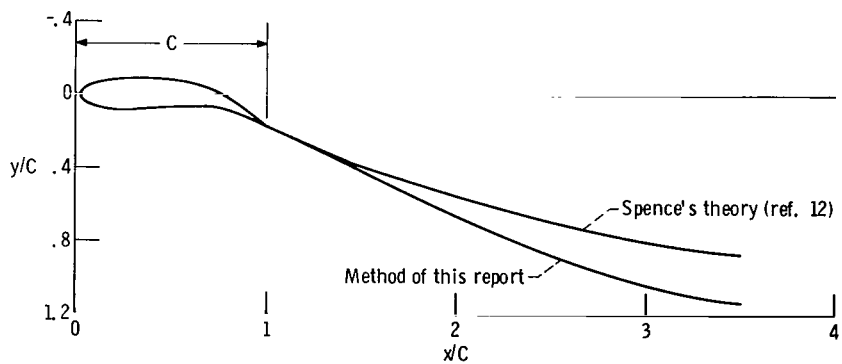


Figure 10. - Comparison of theoretical nondimensional jet shapes. Flap angle, 30° ; thrust coefficient, 3.

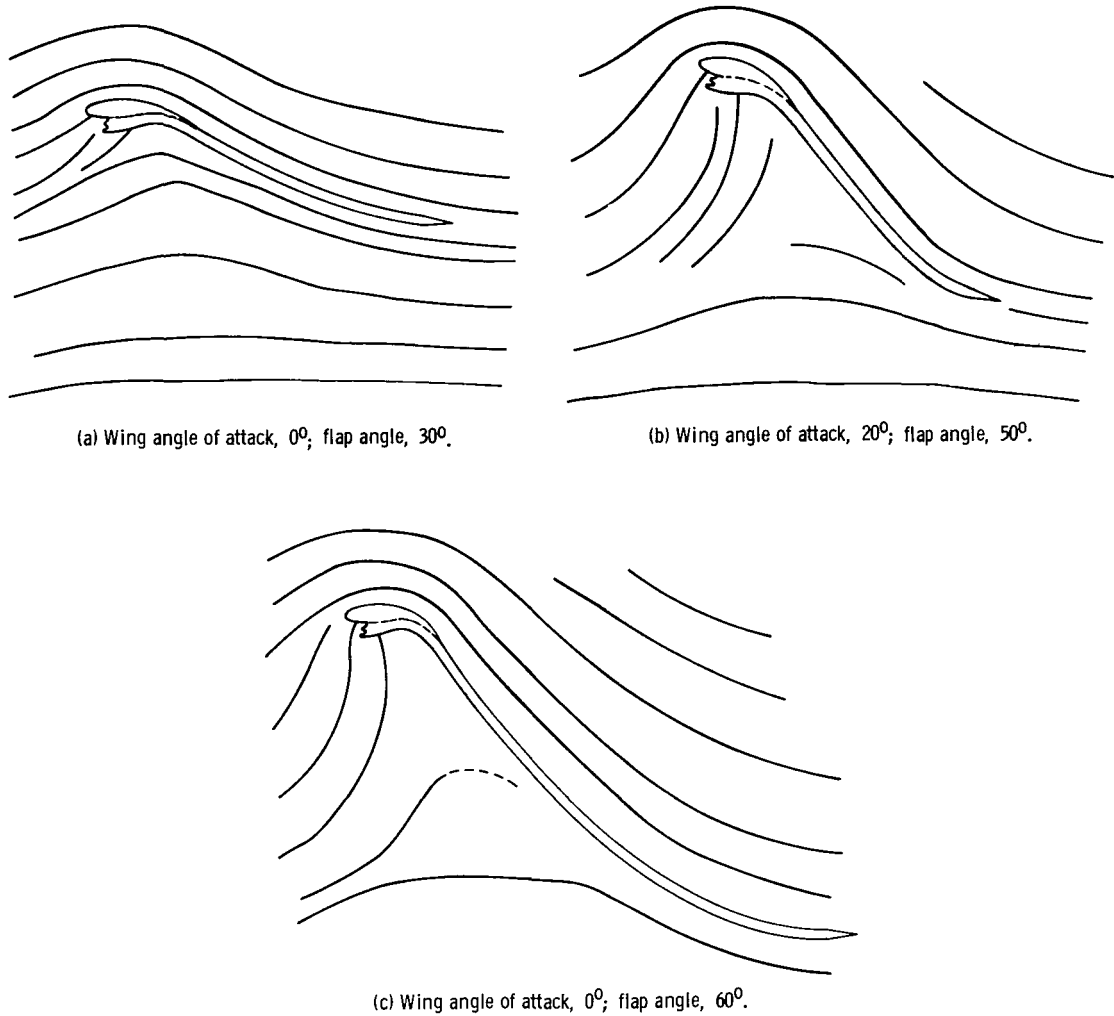


Figure 11. - Flow field for externally blown flap, wing propulsion system. Mass flow coefficient, 0.38; thrust coefficient, 3.

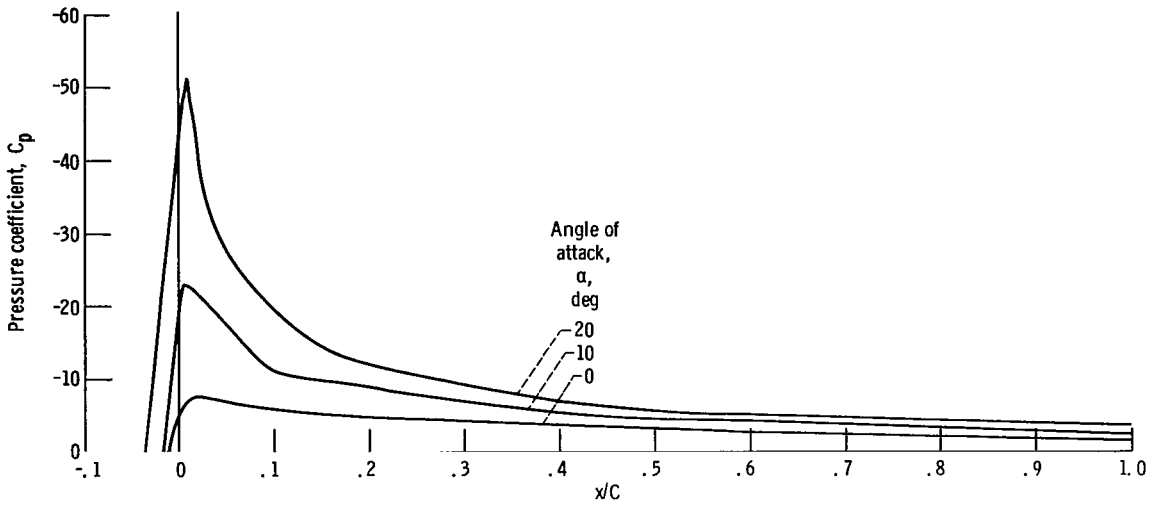


Figure 12. - Calculated pressure distributions on upper surface for fan-wing combination for various angles of attack. Flap angle, 30° ; mass flow coefficient, 0.38; thrust coefficient, 3.

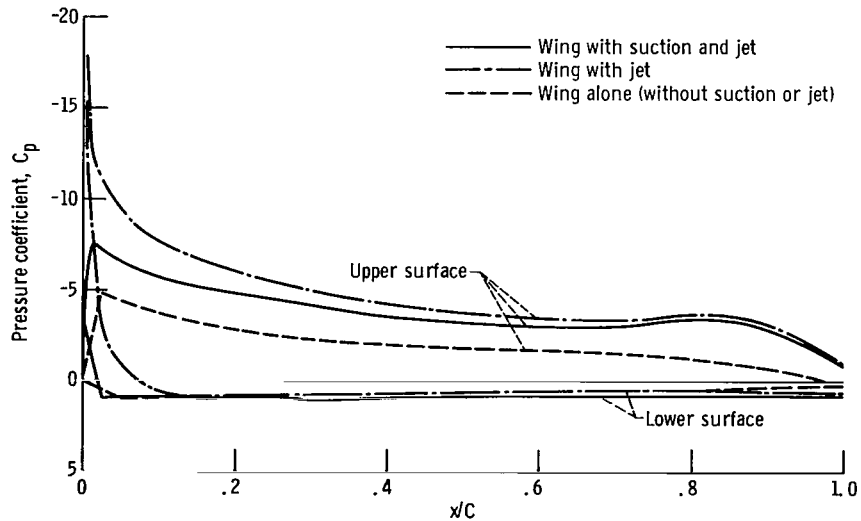


Figure 13. - Effect of suction and jet on pressure distribution. Flap angle, 30° ; angle of attack, 0° .

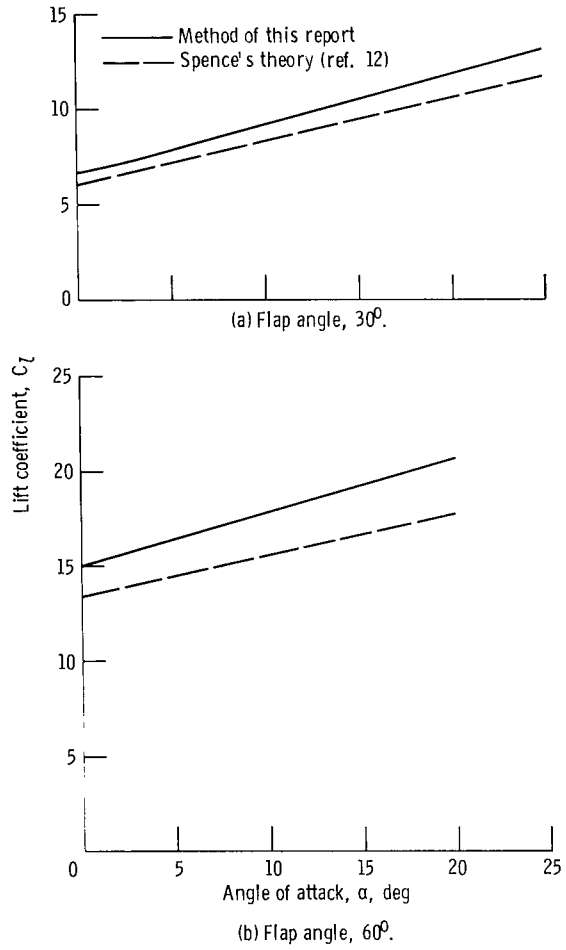


Figure 14. - Comparison of theoretical two-dimensional lift coefficients for blown flap. Thrust coefficient, 3.

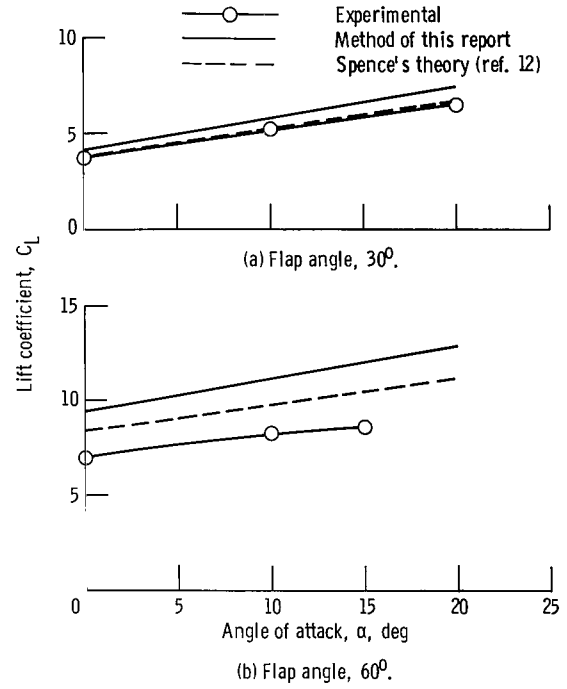


Figure 15. - Comparison of calculated and experimental three-dimensional lift coefficients for blown flap. Thrust coefficient, 3.

NATIONAL AERONAUTICS AND SPACE ADMINISTRATION

WASHINGTON, D. C. 20546

OFFICIAL BUSINESS

PENALTY FOR PRIVATE USE \$300

FIRST CLASS MAIL



POSTAGE AND FEES PAID
NATIONAL AERONAUTICS AND
SPACE ADMINISTRATION

07U 001 26 51 3DS 71166 00903
AIR FORCE WEAPONS LABORATORY /WLOL/
KIRTLAND AFB, NEW MEXICO 87117

ATT E. LOU BOWMAN, CHIEF, TECH. LIBRARY

POSTMASTER: If Undeliverable (Section 158
Postal Manual) Do Not Return

"The aeronautical and space activities of the United States shall be conducted so as to contribute . . . to the expansion of human knowledge of phenomena in the atmosphere and space. The Administration shall provide for the widest practicable and appropriate dissemination of information concerning its activities and the results thereof."

— NATIONAL AERONAUTICS AND SPACE ACT OF 1958

NASA SCIENTIFIC AND TECHNICAL PUBLICATIONS

TECHNICAL REPORTS: Scientific and technical information considered important, complete, and a lasting contribution to existing knowledge.

TECHNICAL NOTES: Information less broad in scope but nevertheless of importance as a contribution to existing knowledge.

TECHNICAL MEMORANDUMS: Information receiving limited distribution because of preliminary data, security classification, or other reasons.

CONTRACTOR REPORTS: Scientific and technical information generated under a NASA contract or grant and considered an important contribution to existing knowledge.

TECHNICAL TRANSLATIONS: Information published in a foreign language considered to merit NASA distribution in English.

SPECIAL PUBLICATIONS: Information derived from or of value to NASA activities. Publications include conference proceedings, monographs, data compilations, handbooks, sourcebooks, and special bibliographies.

TECHNOLOGY UTILIZATION PUBLICATIONS: Information on technology used by NASA that may be of particular interest in commercial and other non-aerospace applications. Publications include Tech Briefs, Technology Utilization Reports and Technology Surveys.

Details on the availability of these publications may be obtained from:

SCIENTIFIC AND TECHNICAL INFORMATION OFFICE

NATIONAL AERONAUTICS AND SPACE ADMINISTRATION

Washington, D.C. 20546